Nonlinear automatic landing control of unmanned aerial vehicles on moving platforms via a 3D laser radar

Hervas, Jaime Rubio; Reyhanoglu, Mahmut; Tang, Hui

2014

Hervas, J. R., Reyhanoglu, M., & Tang, H. (2014). Nonlinear automatic landing control of unmanned aerial vehicles on moving platforms via a 3D laser radar. AIP Conference Proceedings, 907-917.

https://hdl.handle.net/10356/81916

https://doi.org/10.1063/1.4904663

Nonlinear automatic landing control of unmanned aerial vehicles on moving platforms via a 3D laser radar

Jaime Rubio Hervas, Mahmut Reyhanoglu, and Hui Tang

Citation: AIP Conference Proceedings **1637**, 907 (2014); doi: 10.1063/1.4904663
View online: http://dx.doi.org/10.1063/1.4904663
View Table of Contents: http://scitation.aip.org/content/aip/proceeding/aipcp/1637?ver=pdfcov
Published by the AIP Publishing

Nonlinear Automatic Landing Control of Unmanned Aerial Vehicles on Moving Platforms via a 3D Laser Radar

Jaime Rubio Hervas*, Mahmut Reyhanoglu† and Hui Tang*

*School of Mechanical and Aerospace Engineering
Nanyang Technological University
Singapore, 639798, Republic of Singapore
†Physical Sciences Department
Embry-Riddle Aeronautical University
Daytona Beach, FL 32114, USA

Abstract. This paper presents a motion tracking and control system for automatically landing Unmanned Aerial Vehicles (UAVs) on an oscillating platform using Laser Radar (LADAR) observations. The system itself is assumed to be mounted on a ship deck. A full nonlinear mathematical model is first introduced for the UAV. The ship motion is characterized by a Fourier transform based method which includes a realistic characterization of the sea waves. LADAR observation models are introduced and an algorithm to process those observations for yielding the relative state between the vessel and the UAV is presented, from which the UAV's state relative to an inertial frame can be obtained and used for feedback purposes. A sliding mode control algorithm is derived for tracking a landing trajectory defined by a set of desired waypoints. An extended Kalman filter (EKF) is proposed to account for process and observation noises in the design of a state estimator. The effectiveness of the control algorithm is illustrated through a simulation example.

Keywords: UAV, sliding mode, nonlinear control, state estimation, extended Kalman filter, laser radar, landing.

INTRODUCTION

Landing a UAV on a moving platform has been the focus of considerable research in recent years. Existing methodologies for autonomous landing of UAVs are mostly based on vision techniques. In this regard, the theoretical underpinnings and hands-on methodologies underlying UAV automated landing systems do not reflect current technological capabilities. Although vision techniques have reached maturity in some aspects, they still involve complicated processing procedures which limit their use in real-time applications. This implies that quite a few critical issues should be addressed before even getting to the mere computation of the relative state which is imperative for automated landing. This is why most of the works in this category are applied to rotary-wing UAVs which exhibit mild and nearly stationary motion ([16], [17]). Some rotary-wing UAVs landing on moving platforms using vision-based systems are presented in [10], [12], [15] and [21]. In [3], a laser rangefinder system and a visual tracking sensor are combined to construct a low-cost guidance system for a helicopter. In [6], a nonlinear controller that exploits the measurement of the average optical flow is presented. Nevertheless, due to its computational overhead and limited accuracy, these approaches are mostly applicable for slow moving and not too fast UAVs.

Autonomous vision-based net recovery systems for small fixed-wing UAVs are presented in [4], [7] and [8]. In [25], a videometric method to implement terminal guidance for accurate landing is presented. In [13], a system mounted on the UAV itself uses a laser altimeter and inertial measuring devices for automatic landing. However, all these works assume a stationary (sometimes known) landing pad. Some other works study the problem of landing on a ship deck [14] using cooperative infrared object on the runway and the infrared computer vision on the UAV ([22], [24]).

This paper studies the problem of automatically landing a UAV on an oscillating platform such as a ship deck using LADAR observations. It is organized as follows. In Sections II, III, and IV, mathematical models for the UAV and the vessel are presented. Section V introduces a LADAR observation model and an algorithm to determine the relative state between the vessel and the UAV. A statistical method is used to account for the multiple observations available. Based on the available measurements and given the inherent difficulties of an exact tracking of the ship dynamics, a sliding mode control algorithm is proposed in Section VI for tracking a landing trajectory defined by a set of desired waypoints. In Section VII, state estimation is carried out by an EKF which also accounts for the presence of noise. A net is assumed to be available for recovery purposes in Section VIII. Finally, in Section IX, the effectiveness of the

10th International Conference on Mathematical Problems in Engineering, Aerospace and Sciences
AIP Conf. Proc. 1637, 907-917 (2014); doi: 10.1063/1.4904663

control algorithm is illustrated through a simulation example.

PRELIMINARIES

Let us denote by F_o the Earth-fixed frame (considered inertial under the hypothesis of flat and fixed Earth), F_b the UAV-fixed body frame, and F_s the vessel-fixed body frame. Standard definitions of these frames can be found in [1] and [19]. The superscripts "s" and "b" will be used to distinguish the motion variables for the ship and the UAV whenever necessary. For simplicity, in the individual sections, where the equations of motion (EOMs) for the UAV and the ship are derived separately, these superscripts are dropped. The abbreviations $\mathrm{s}(\cdot) = \sin(\cdot)$, $\mathrm{c}(\cdot) = \cos(\cdot)$, and $\mathrm{t}(\cdot) = \tan(\cdot)$ are used throughout the paper.

AIRCRAFT DYNAMICS

Equations of motion for the UAV are widely available in the literature ([1], [2]). The EOMs are obtained for the translational and rotational motion assuming no wind condition.

Translational Equations of Motion

The translational EOMs for an aircraft of mass m can be written as follows:

$$\dot{x} = V\mathrm{c}\gamma_2\mathrm{c}\gamma_3 \tag{1}$$
$$\dot{y} = V\mathrm{c}\gamma_2\mathrm{s}\gamma_3 \tag{2}$$
$$\dot{h} = V\mathrm{s}\gamma_2 \tag{3}$$
$$m\dot{V} = -D + T\mathrm{c}\alpha\mathrm{c}\beta - mg\mathrm{s}\gamma_2 \tag{4}$$
$$mV\dot{\gamma}_3\mathrm{c}\gamma_2 = Y\mathrm{c}\gamma_1 + L\mathrm{s}\gamma_1 - T(\mathrm{c}\alpha\mathrm{s}\beta\mathrm{c}\gamma_1 - \mathrm{s}\alpha\mathrm{s}\gamma_1) \tag{5}$$
$$mV\dot{\gamma}_2 = -Y\mathrm{s}\gamma_1 + L\mathrm{c}\gamma_1 - mg\mathrm{c}\gamma_2 + T(\mathrm{c}\alpha\mathrm{s}\beta\mathrm{s}\gamma_1 + \mathrm{s}\alpha\mathrm{c}\gamma_1) \tag{6}$$

where V denotes the velocity of the aircraft's center of mass; (x, y, h) are the inertial coordinates (range, lateral displacement and altitude) of the aircraft's center of mass; (D, T, L, Y) are the drag, thrust, lift, and side forces; g is the gravitational acceleration; and $(\gamma_1, \gamma_2, \gamma_3)$ denote the bank, climb and track angles, respectively. The angle of attack and sideslip angle are denoted by α and β, respectively.

Rotational Equations of Motion

Let (x_b, y_b, z_b) denote the aircraft-fixed principal axes, where x_b is the longitudinal axis, y_b is the lateral axis, and z_b is the directional axis. Moreover, assume that x_b-z_b is the symmetry plane. Then, the rotational EOMs can be written as follows:

$$\begin{bmatrix} \dot{\phi} \\ \dot{\theta} \\ \dot{\psi} \end{bmatrix} = \begin{bmatrix} 1 & \mathrm{s}\phi\mathrm{t}\theta & \mathrm{c}\phi\mathrm{t}\theta \\ 0 & \mathrm{c}\phi & -\mathrm{s}\phi \\ 0 & \frac{\mathrm{s}\phi}{\mathrm{c}\theta} & \frac{\mathrm{c}\phi}{\mathrm{c}\theta} \end{bmatrix} \begin{bmatrix} p \\ q \\ r \end{bmatrix} \tag{7}$$

$$\begin{bmatrix} \dot{p} \\ \dot{q} \\ \dot{r} \end{bmatrix} = \mathbf{I}^{-1} \begin{bmatrix} \mathscr{L} - (I_z - I_y)qr + I_{xz}pq - qh'_z + rh'_y \\ \mathscr{M} + Td_T + (I_z - I_x)pr - I_{xz}\left(p^2 - r^2\right) - rh'_x + ph'_z \\ \mathscr{N} - (I_y - I_x)pq - I_{xz}qr - ph'_y + qh'_x \end{bmatrix} \tag{8}$$

where

$$\mathbf{I} = \begin{bmatrix} I_x & 0 & -I_{xz} \\ 0 & I_y & 0 \\ -I_{xz} & 0 & I_z \end{bmatrix} \tag{9}$$

is the inertia matrix and (ϕ, θ, ψ) denotes the roll, pitch, and yaw angles; (p, q, r) is the angular velocity vector; (h'_x, h'_y, h'_z) denotes the angular momentum vector of all rotors about the aircraft-fixed x_b, y_b, z_b axes; $(\mathscr{L}, \mathscr{M}, \mathscr{N})$ is the moment vector (rolling, pitching, and yawing moments); (I_x, I_y, I_z) are moments of inertia about the aircraft-fixed x_b, y_b, z_b axes; and I_{xz} denotes the product of inertia. It will be assumed that the line of action of the thrust is contained in the aircraft vertical plane at a distance d_T of its center of mass. Throughout the paper, 321 Euler angle sequence is used, so that $|\theta| < \pi/2$.

Other Relationships

The angles γ_i $(i = 1, 2, 3)$, α and β, are defined as follows:

$$\alpha = \mathrm{t}^{-1}\frac{w}{u}, \quad \beta = \mathrm{s}^{-1}\frac{v}{V} \tag{10}$$

$$\gamma_1 = \mathrm{s}^{-1}\frac{\mathrm{c}\alpha\mathrm{s}\beta\mathrm{s}\theta + \mathrm{c}\beta\mathrm{s}\phi\mathrm{c}\theta - \mathrm{s}\alpha\mathrm{s}\beta\mathrm{c}\phi\mathrm{c}\theta}{\mathrm{c}\gamma_2} \tag{11}$$

$$\gamma_2 = -\mathrm{s}^{-1}\frac{\dot{h}}{V}, \quad \gamma_3 = \mathrm{s}^{-1}\frac{\dot{y}}{V\mathrm{c}\gamma_2} \tag{12}$$

The velocity can be expressed as follows:

$$\begin{bmatrix} u \\ v \\ w \end{bmatrix} = V\mathbf{T}_{bo}\begin{bmatrix} \mathrm{c}\gamma_2\mathrm{c}\gamma_3 \\ \mathrm{c}\gamma_2\mathrm{s}\gamma_3 \\ -\mathrm{s}\gamma_2 \end{bmatrix} \tag{13}$$

where the transformation matrix from the inertial to the body frame is given by:

$$\mathbf{T}_{bo} = \begin{bmatrix} \mathrm{c}\theta\mathrm{c}\psi & \mathrm{c}\theta\mathrm{s}\psi & -\mathrm{s}\theta \\ \mathrm{s}\phi\mathrm{s}\theta\mathrm{c}\psi - \mathrm{c}\phi\mathrm{s}\psi & \mathrm{s}\phi\mathrm{s}\theta\mathrm{s}\psi + \mathrm{c}\phi\mathrm{c}\psi & \mathrm{s}\phi\mathrm{c}\theta \\ \mathrm{c}\phi\mathrm{s}\theta\mathrm{c}\psi + \mathrm{s}\phi\mathrm{s}\psi & \mathrm{c}\phi\mathrm{s}\theta\mathrm{s}\psi - \mathrm{s}\phi\mathrm{c}\psi & \mathrm{c}\phi\mathrm{c}\theta \end{bmatrix}$$

For a truly symmetric configuration, it is common to neglect:

- all the derivatives of the asymmetric or lateral forces and moments with respect to the symmetric or longitudinal motion variables,
- all the derivatives of the symmetric forces and moments with respect to the asymmetric motion variables.

Thus, the aerodynamic forces and moments can be expressed as follows:

$$L = QS\left(C_{L_0} + C_{L_\alpha}\alpha\right) \tag{14}$$

$$D = QS\left(C_{D_0} + k_1 C_L + k_2 C_L^2\right) \tag{15}$$

$$\mathscr{M} = QSc\left(C_{m_0} + C_{m_\alpha}\alpha + C_{m_{\delta_e}}\delta_e + \frac{c}{2}C_{m_q}q\right) \tag{16}$$

$$Y = QS\left(C_{Y_\beta}\beta + C_{Y_{\delta_r}}\delta_r + \frac{b}{2V}\left(C_{Y_p}p + C_{Y_r}r\right)\right) \tag{17}$$

$$\mathscr{L} = QSb\left(C_{l_\beta}\beta + C_{l_{\delta_a}}\delta_a + C_{l_{\delta_r}}\delta_r + \frac{b}{2V}\left(C_{l_p}p + C_{l_r}r\right)\right) \tag{18}$$

$$\mathscr{N} = QSb\left(C_{n_\beta}\beta + C_{n_{\delta_a}}\delta_a + C_{n_{\delta_r}}\delta_r + \frac{b}{2V}\left(C_{n_p}p + C_{n_r}r\right)\right) \tag{19}$$

where $Q = 1/2\rho V^2$ is the dynamic pressure, ρ stands for the air density, S is the wing surface, c is the mean aerodynamic chord, b is the wing span, and $(\delta_a, \delta_e, \delta_r)$ denotes the aileron, elevator, and rudder deflections.

A simple model is generally used to define the modulus of thrust for a propeller propulsion engine as follows:

$$T = \frac{k_m\rho}{V}\eta \tag{20}$$

where k_m is a constant and η represents the position of the throttle (between 0 and 1 inclusive).

Compact Form

Defining the state and control vectors as $\hat{\boldsymbol{\xi}} = [x, y, h, V, \gamma_2, \gamma_3, \phi, \theta, \psi, p, q, r]^T$ and $\hat{\mathbf{u}} = [\eta, \delta_a, \delta_e, \delta_r]$, respectively; the system above can be expressed as follows:

$$\dot{\hat{\boldsymbol{\xi}}} = \hat{\mathbf{f}}(\hat{\boldsymbol{\xi}}) + \hat{\mathbf{g}}(\hat{\boldsymbol{\xi}})\hat{\mathbf{u}} \tag{21}$$

SHIP MOTION

The motion of a marine vessel can be described in terms of 6 degrees-of-freedom: surge (longitudinal motion in the horizonal plane, X), sway (sideways motion in the horizonal plane, Y), heave (vertical motion, Z), roll (rotation about the longitudinal axes, Φ), pitch (rotation about the transverse axis, Θ), and yaw (rotation about the vertical axes, Ψ). Standard definitions can be found in [19]. The position-orientation (i.e., state) vector $\boldsymbol{\chi}$ expressed in the inertial frame can be written as:

$$\boldsymbol{\chi} = [X, Y, Z, \Phi, \Theta, \Psi]^T \tag{22}$$

A simple method suitable for accurate simulation that incorporates parameters related to the recommended spectral family and particular vehicle model is presented in [11], where given the motion spectrum, a finite sum of sinusoidal components with a random initial phase ε_j is proposed to simulate the motion of a ship as:

$$\chi_i(t) = \sum_{j=1}^{N} \bar{\chi}_{ij} \cos(\omega_{ej} t + \varepsilon_j) \tag{23}$$

where ω_{ej} is the encounter frequency of the individual components and $\bar{\chi}_{ij}$ is a parameter depending on the geometry of the hull and load conditions of the vessel. Details on how to calculate those values can be found in [11].

For simplicity, it will be assumed that the LADAR frame coincides with the vessel frame and its motion can be described by (23). This assumption can be easily relaxed.

LADAR OBSERVATION MODEL

LADAR technology consists of a modulated laser emitter coupled with a focal plane array detector and the required optics. This sensor creates an "image" of the environment by producing a 2D image where each pixel has an associated range and intensity value. A typical algorithm first converts the 3D imaging sensor measurements to a 3D point cloud, and then significant environmental features such as planar, line or point features are extracted and associated from one 3D imaging sensor frame to the next. Finally, characteristics of these features such as the direction vectors are used to compute the platform position and attitude changes. In this paper, it will be assumed that a set of N points Q_i ($i = 1, \ldots, N$) are identified by the LADAR at every time step (given by its sampling rate) based on their reflectance characteristics and that those points can be identified from one frame to the other.

Let us denote by $\mathbf{r}_{iL}$ and $\mathbf{r}_{O_bL}$ the position vectors of a point Q_i on the aircraft and the origin of the aircraft body frame O_b with respect to the LADAR, respectively; and $\mathbf{r}_{iO_b}$ the position vector from O_b to Q_i (see Fig. 1). Then, the following equations can be written:

$$\mathbf{r}^s_{O_bL} + \mathbf{T}_{sb}\mathbf{r}^b_{iO_b} = \mathbf{r}^s_{iL}, \quad \forall i \tag{24}$$

where $\mathbf{T}_{sb}$ represents the rotation matrix from the UAV-fixed body frame to the LADAR frame. It is to be noted that, in equation (24), $\mathbf{r}^s_{iL}$ is known from the LADAR observations (the time delay between the emitted and received beam provides information of the distance of point Q_i to the LADAR and its orientation since the orientation of the beam is known), and $\mathbf{r}^b_{iO_b}$ is also known since the geometry of the aircraft is assumed to be known; however, $\mathbf{r}^s_{O_bL}$ is not known a priori.

Subtracting equations (24) yields

$$\mathbf{T}_{sb}\mathbf{a}^b_{ij} = \mathbf{b}^s_{ij}, \quad \forall i, j, \quad i \neq j \tag{25}$$

where $\mathbf{a}^b_{ij} = \mathbf{r}^b_{iO_b} - \mathbf{r}^b_{jO_b}$ and $\mathbf{b}^s_{ij} = \mathbf{r}^s_{iL} - \mathbf{r}^s_{jL}$.

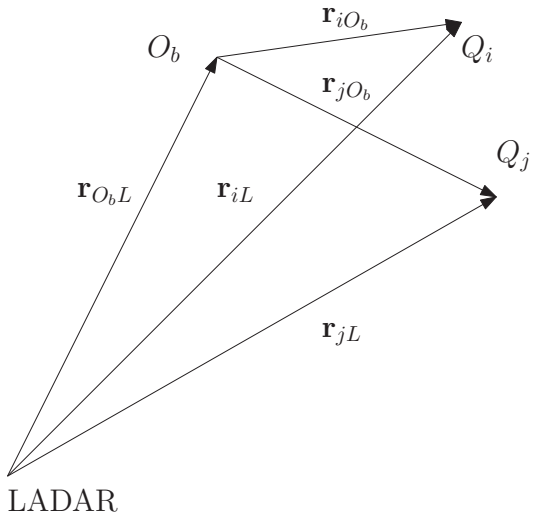

Figure 1. Relations between points on the aircraft and their LADAR observations.

Since usually $M > 2$ observations are available, a statistical method can be applied to make use of all the information. One way to state the problem is finding a matrix $\mathbf{T}_{sb}$ that minimizes the loss function J defined as:

$$J(\mathbf{T}_{sb}) = \frac{1}{2}\sum_{l=1}^{M} w_l \mid \mathbf{b}_l^s - \mathbf{T}_{sb}\mathbf{a}_l^b \mid^2 \tag{26}$$

where w_l denote the weightings. Different methods are available in the literature for solving this minimization problem. In this paper, an exact method known as the "q-method" is chosen. The details of this method can be found in [23].

Once the relative orientation matrix $\mathbf{T}_{sb}$ has been estimated, equation (24) provides the position of the origin of the UAV-fixed body frame with respect to the LADAR. As a first approach, the average of all available measurements is considered, i.e.,

$$\mathbf{r}_{O_bL}^s = \frac{1}{N}\sum_{i=1}^{N}(\mathbf{r}_{iL}^s - \mathbf{T}_{sb}\mathbf{r}_{iO_b}^b) \tag{27}$$

Finally, the dynamics of the UAV can be recovered from:

$$[x^o, y^o, h^o]^T = \mathbf{T}_{os}\mathbf{r}_{O_bL}^s + [X^o, Y^o, -Z^o]^T \tag{28}$$

where $\mathbf{T}_{os}$ is the rotation matrix from the LADAR to the inertial frame and is assumed to be known, and

$$\phi = \mathrm{t}^{-1}\frac{T_{bo_{23}}}{T_{bo_{33}}}, \quad \theta = -\mathrm{s}^{-1}T_{bo_{13}}, \quad \psi = \mathrm{t}^{-1}\frac{T_{bo_{12}}}{T_{bo_{11}}} \tag{29}$$

where $\mathbf{T}_{bo} = \mathbf{T}_{bs}\mathbf{T}_{so}$ and $T_{bo_{ij}}$ denotes the component in the i-th row and j-th column in the matrix $\mathbf{T}_{bo}$.

Since these estimations are made at a constant sampling frequency, they can be discretized at every time step t_k. Then, using a simple Euler discretization algorithm, the observation vector can be defined as:

$$\boldsymbol{\eta}_k = [\dot{x}^o, \dot{y}^o, \dot{h}^o, \phi, \theta, \psi, \dot{\phi}, \dot{\theta}, \dot{\psi}]_k^T \tag{30}$$

and used for feedback purposes.

CONTROL ALGORITHM

The landing problem is now formulated into a trajectory tracking problem where the control objective is to make the system seek known references in the state variables $\hat{\boldsymbol{\xi}}$ using the control input vector $\hat{\mathbf{u}}$. It is to be noted that EOMs (21) are nonlinear, but affine in control input for the chosen aircraft model. Two different controllers are proposed: the velocity is exclusively controlled using the position of the throttle η and the rest of the dynamics are controlled using the aileron (δ_a), elevator (δ_e), and rudder (δ_r) angles. It will be assumed that the state $\hat{\boldsymbol{\xi}}$ is measurable.

Velocity Control

Denote by V_d a reference velocity and define the error $e_V := V - V_d$. Then, combining equations (4), (14), (15), and (20), the evolution of the error becomes:

$$\dot{e}_V = -\frac{D(e_V + V_d, \alpha)}{m} + \frac{k_m \rho}{m(e_V + V_d)} \eta \mathrm{c}\alpha \mathrm{c}\beta - g\mathrm{s}\gamma_2 - \dot{V}_d \tag{31}$$

It can be easily seen that the feedback law given by:

$$\eta = \frac{e_V + V_d}{k_m \rho} \frac{m}{\mathrm{c}\alpha \mathrm{c}\beta} \left(g\mathrm{s}\gamma_2 + \dot{V}_d + \frac{\rho S}{2m}(e_V + V_d)^2 C_D(\alpha) - k_V e_V \right) \tag{32}$$

where k_V is a positive constant, guarantees convergence of e_V to zero. Note that the range equation (1) is closely related to the velocity and it does not present much interest from the control point of view.

Sliding Mode Controller

The state equations (21) with state and control input vectors given by:

$$\boldsymbol{\xi} = [y, h, \gamma_2, \gamma_3, \phi, \theta, \psi, p, q, r]^T \tag{33}$$

$$\mathbf{u} = [\delta_a, \delta_e, \delta_r]^T \tag{34}$$

can be rewritten as:

$$\dot{\boldsymbol{\xi}} = \mathbf{f}(\boldsymbol{\xi}) + \mathbf{g}(\boldsymbol{\xi})\mathbf{u} \tag{35}$$

Define the set of sliding functions as:

$$\mathbf{s} = \begin{bmatrix} \lambda_{\dot{\phi}} \left(\dot{\phi} - \dot{\phi}_d \right) + \lambda_{\phi} \left(\phi - \phi_d \right) \\ \lambda_{\dot{\theta}} \left(\dot{\theta} - \dot{\theta}_d \right) + \lambda_{\theta} \left(\theta - \theta_d \right) \\ \lambda_{\psi} \left(\dot{\psi} - \dot{\psi}_d \right) + \lambda_{\psi} \left(\psi - \psi_d \right) \end{bmatrix} \tag{36}$$

where λ_{ϕ}, λ_{θ}, λ_{ψ}, $\lambda_{\dot{\phi}}$, $\lambda_{\dot{\theta}}$, and $\lambda_{\dot{\psi}}$ are positive constants. It is assumed that for system (35) under definition (36), the matrix $\frac{\partial \mathbf{s}}{\partial \boldsymbol{\xi}} \mathbf{g}(\boldsymbol{\xi})$ is non-singular. This assumption has been verified through simulations.

The actual reference trajectory the aircraft is required to track is given by:

$$y = y_d, \quad h = h_d \tag{37}$$

Without loss of generality, it is assumed that $y_d = h_d = 0$. To make the above reference flight path a solution to the sliding functions, the spatial errors are transcribed into the desired state variables through the following transformation:

$$\begin{bmatrix} \phi_d \\ \theta_d \\ \psi_d \end{bmatrix} = \begin{bmatrix} 0 \\ \alpha_0 + \gamma_{2_d} \\ \gamma_{3_d} \end{bmatrix} \tag{38}$$

where, based on equations (2) and (3),

$$\gamma_{2_d} = -\mathrm{s}^{-1}\left(k_{\gamma_2} h\right), \quad \gamma_{3_d} = -\mathrm{s}^{-1}\left(k_{\gamma_3} y\right) \tag{39}$$

and where α_0 denotes the trim angle of attack (assumed to be known), k_{γ_2} and k_{γ_3} are sufficiently small positive constants, and k is a positive constant.

Define now a positive definite Lyapunov functional in terms of the sliding functions (36) as:

$$E = \frac{1}{2}\mathbf{s}^T \mathbf{s} \tag{40}$$

which derivative yields:

$$\dot{E} = \mathbf{s}^T \dot{\mathbf{s}} = \mathbf{s}^T \frac{\partial \mathbf{s}}{\partial \boldsymbol{\xi}} \dot{\boldsymbol{\xi}} = \mathbf{s}^T \frac{\partial \mathbf{s}}{\partial \boldsymbol{\xi}} [\mathbf{f}(\boldsymbol{\xi}) + \mathbf{g}(\boldsymbol{\xi})\mathbf{u}] \tag{41}$$

Then, for a control law of the form:

$$\mathbf{u} = -\left(\frac{\partial \mathbf{s}}{\partial \boldsymbol{\xi}} \mathbf{g}(\boldsymbol{\xi})\right)^{-1} \left[\frac{\partial \mathbf{s}}{\partial \boldsymbol{\xi}} \mathbf{f}(\boldsymbol{\xi}) + \mathbf{K}\mathbf{s}\right] \tag{42}$$

the time derivative of the Lyapunov functional can be rewritten as:

$$\dot{E} = -\mathbf{s}^T \mathbf{K}\mathbf{s} \tag{43}$$

which is negative definite for a positive definite $\mathbf{K}$ matrix. This guarantees convergence of the roll, pitch and yaw angles to their desired values (38). By construction of the sliding manifold, it can be easily shown that γ_2 and γ_3 will converge to their desired values γ_{2_d} and γ_{3_d}, respectively; which by definitions (39) together with equations (2)-(3) implies

$$\dot{y} = -V c \gamma_2 k_{\gamma_3} y \tag{44}$$

$$\dot{h} = -V k_{\gamma_2} h \tag{45}$$

A similar Lyapunov approach to the one above can be used to subsequently ensure convergence of the inertial coordinates y and h to their desired values (i.e., the origin), and thus convergence of the actual trajectory to the desired one (37) is guaranteed.

It is to be noted that the computed control inputs are subject to saturation and rate limits. Gains can be appropriately changed to achieve a satisfactory performance.

NOISE ADDITION AND FILTERING

A state estimation is required to implement the control laws (32) and (42). In this paper, an EKF is proposed that also accounts for the noise. Implementation details can be widely found in literature (e.g. [18]).

Define the random variable $\mathbf{w}$ representing the process noise, then (21) can be written as

$$\dot{\hat{\boldsymbol{\xi}}} = \hat{\mathbf{f}}(\hat{\boldsymbol{\xi}}) + \hat{\mathbf{g}}(\hat{\boldsymbol{\xi}})\hat{\mathbf{u}} + \mathbf{w} \tag{46}$$

Given an output vector $\boldsymbol{\eta}$ and measurement noise vector $\mathbf{v}$, the observation equation can be written as

$$\boldsymbol{\eta} = \mathbf{h}(\hat{\boldsymbol{\xi}}) + \mathbf{v} \tag{47}$$

Equations (46) together with (47) describe the system required for EKF implementation. It is assumed that $\mathbf{w}$ and $\mathbf{v}$ are white gaussian noises with covariance matrices $\mathbf{Q}$ and $\mathbf{R}$, respectively.

RECOVERY

Recovery is defined as transitioning the UAV from a flying state to a nonflying one. Different methods available are illustrated in [5]. In this paper, a net is assumed to be available on the vessel such that is centered at the desired trajectory given by (37) for the boat at a reference position. Its size is determined such that for a given wingspan (b), safety margin (SM) and sea state (described in terms of maximum vertical $H_{\max}$ and horizontal $Y_{\max}$ vessel displacement with respect to the previous reference position), the tracking trajectory is always included in the net. Then, L_{net} and W_{net} define the net size as:

$$L_{\text{net}} = (2Y_{\max} + b)SM, \quad W_{\text{net}} = (2H_{\max} + b)SM \tag{48}$$

SIMULATIONS

The feedback control law developed in the previous section is implemented here. The physical parameters used in the simulations (given in Table 1) correspond to actual values of the Lambda Unmanned Research Vehicle [20] except for the inertia values. The saturation limits are assumed to be:

$$| \delta_a | \leq 30^o, \quad | \delta_e | \leq 30^o, \quad | \delta_r | \leq 30^o, \quad 0 \leq \eta \leq 1$$

Here it is assumed that angular momentum of the rotors are negligible and that the point of application of the thrust is along the body frame longitudinal axis (i.e., $d_T = 0$).

Table 1. Parameters for the Lambda UAV landing at sea level [20].

Parameter	Value	Parameter	Value	Parameter	Value	Parameter	Value
ρ	$1.225\,\mathrm{kg/m^3}$	m	$92.10\,\mathrm{kg}$	I_x	$83.75\,\mathrm{kg\cdot m^2}$	I_y	$137.43\,\mathrm{kg\cdot m^2}$
I_z	$210.99\,\mathrm{kg\cdot m^2}$	I_{xz}	$3.05\,\mathrm{kg\cdot m^2}$	S	$1.96\,\mathrm{m^2}$	b	$4.29\,\mathrm{m}$
c	$0.46\,\mathrm{m}$	C_{L_0}	0.7939	C_{L_α}	5.8200	C_{D_0}	0.0290
k_1	0	k_2	0.0363	C_{m_0}	0	C_{m_α}	−1.1010
$C_{m_{\delta_e}}$	−0.8449	C_{m_q}	−15.4000	C_{Y_β}	−0.4372	$C_{Y_{\delta_r}}$	0.2865
C_{Y_p}	−0.0016	C_{Y_r}	0.2601	C_{l_β}	−0.0145	$C_{l_{\delta_a}}$	0.2608
$C_{l_{\delta_r}}$	0.0022	C_{l_p}	−0.5538	C_{l_r}	0.0876	C_{n_β}	0.0600
$C_{n_{\delta_a}}$	−0.0137	$C_{n_{\delta_r}}$	−0.0943	C_{n_p}	−0.0360	C_{n_r}	−0.1650

The landing platform is assumed to be a barge with zero forward speed and a heading angle of 135 deg. For an irregular sea described by Modified Pierson-Moskowits spectrum with a significant wave height $h_{1/3} = 4$ m and dominant wave period $T = 7$ s, the barge motion is shown in Fig. 2.

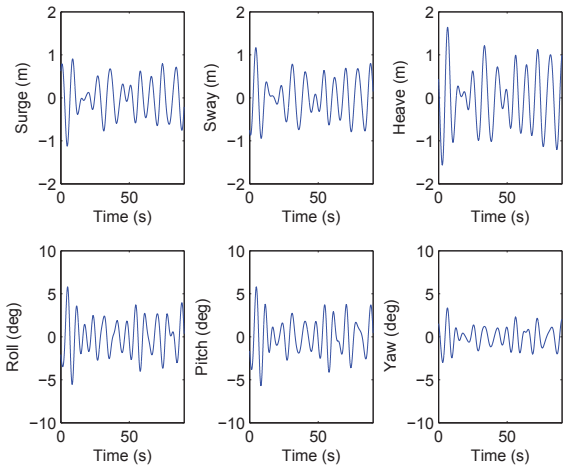

Figure 2. Surge, sway, heave, roll, pitch and yaw motions for a barge at 0 kts and heading angle of 135 deg (sea state described by Modified Pierson-Moskowits spectrum with $h_{1/3} = 4$ m and $T = 7$ s).

A highly dense cloud of points is typically expected to be obtained from the LADAR. For simulation purposes, $N = 38$ points have been considered as shown in Fig. 3. It has been assumed that UAV observations are made as far as 2000 m at a scan rate of 100 Hz (i.e., $\Delta t = 0.01$ s) with an accuracy of 15 cm (one standard deviation). These values reflect state of the art technologies (e.g. Leica LAS60 Airborne Laser Scanner [9]).

The equilibrium initial conditions are taken as:

$$(y, h)_0 = (5, 15)\,\mathrm{m} \quad V_0 = 26.14\,\mathrm{m/s}, \quad (\phi, \theta, \psi)_0 = (15, 3, -15)^o$$

The control objective is to track a trajectory defined by $(y, h)_d = (0, 0)$ and $V_d = 22.22$ m/s. It is to be noted that for this flight condition, the trim angle of attack is $\alpha_0 = 7.11^o$.

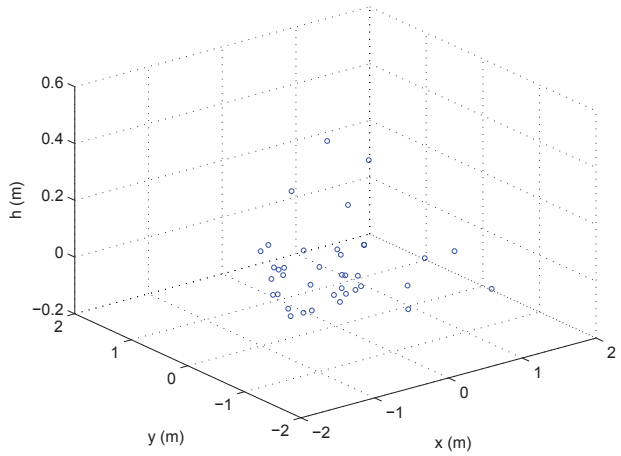

Figure 3. Cloud of points (centered at the UAV center of mass) observed by the LADAR.

The effectiveness of the controller (32) and (42) is demonstrated by applying it to the complete nonlinear system (1)-(6) and (7)-(8). The control parameters are chosen as:

$$k_{\gamma_2} = 0.05, \quad k_{\gamma_3} = 0.05, \quad k_V = 10, \quad \lambda_\phi = \lambda_\theta = \lambda_\psi = 3, \quad \lambda_{\dot\phi} = \lambda_{\dot\theta} = \lambda_{\dot\psi} = 0.5, \quad \mathbf{K} = \text{diag}\{1, 0.1, 5\}$$

It has been assumed that control commands are sent to the servos every 0.1 s.

Zero-mean process (gaussian) noises with a standard deviation of 0.005 are assumed for the variables $[V, \gamma_2, \gamma_3, p, q, r]^T$. For the LADAR measurements, a standard deviation of 0.15 has been assumed. Consequently, the following covariance matrices have been defined:

$$\mathbf{Q} = 0.005^2\,\text{diag}\{1, 1, 1, 0, 0, 0, 1, 1, 1\}$$

$$\mathbf{R} = 10(0.15)^2\,\text{diag}\left\{\frac{10}{\Delta t}, \frac{10}{\Delta t}, \frac{10}{\Delta t}, 1, 1, 1, \frac{1}{\Delta t}, \frac{1}{\Delta t}, \frac{1}{\Delta t}\right\}$$

As can be seen in Figs. 4-5, the state converges to the desired state in about 50 s. Based on the motion of the barge in the vertical plane (see Fig. 2), a safety margin $SM = 1.25$ can be applied to equation (48) such that a net size of 8.25×9.5 m^2 can be used for safe recovery.

CONCLUSION

Based on a full nonlinear mathematical model for the UAV and a Fourier transform based method to describe the ship dynamics, the relative state between the vessel and the UAV has been estimated using LADAR observations. A statistical method has been used to account for the multiple observations available. It has been shown that the UAV state with respect to an inertial frame can be obtained and used for feedback purposes. A sliding mode control algorithm has been designed to track a landing trajectory defined by a set of desired waypoints and an EKF has been introduced to account for the process and observation noises as well as for state estimation purposes. The design of the motion tracking and control system for automatically landing UAVs has been illustrated through a simulation example.

The many avenues considered for future research include the design of control laws that achieve robustness, insensitivity to system and control parameters, and improved disturbance rejection. Estimation of the system and control parameters is expected to be addressed in future research. Future research also includes the development of tracking algorithms for more complex landing trajectories with applications to real-time systems. Nonlinear description of the aerodynamic forces and moments presents another promising avenue of research.

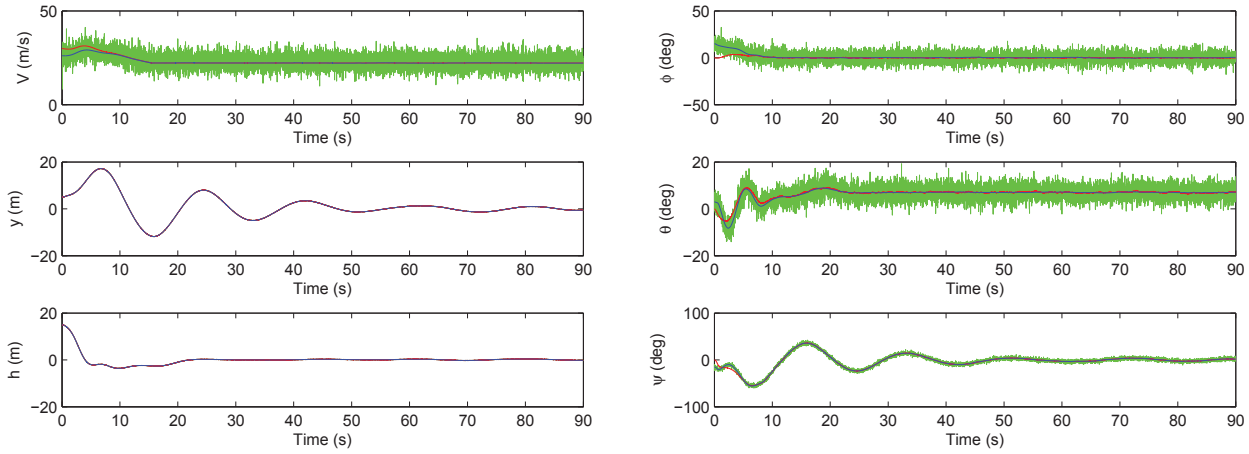

Figure 4. Time responses of the velocity (V), lateral displacement (y), altitude (h), roll (ϕ), pitch (θ) and yaw (ψ) angles. Blue, green and red denote actual, estimated and filtered values, respectively.

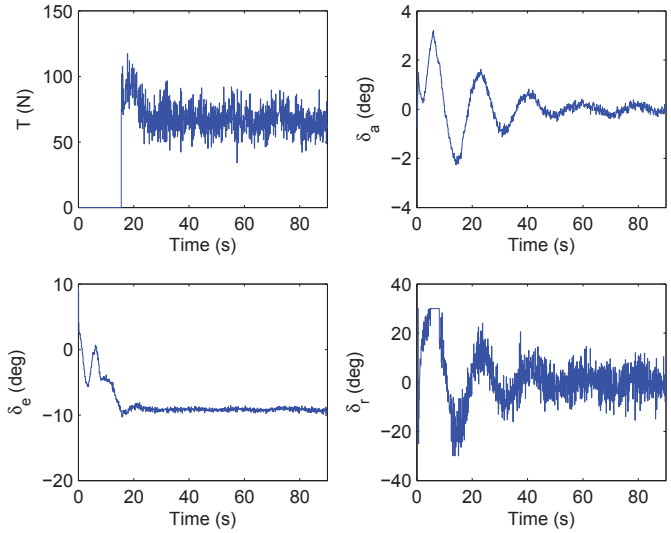

Figure 5. Time responses of the thrust (T), aileron (δ_a), elevator (δ_e) and rudder (δ_r) deflections.

ACKNOWLEDGMENTS

The authors would like to thank the support provided by Nanyang Technological University.

REFERENCES

1. J. L. Boiffier, *The Dynamics of Flight: Equations* (John Wiley & Sons, 1998).
2. M. E. Eshelby, *Aircraft Performance: Theory and Practice* (AIAA Education Series, 2000).
3. M. Garratt, H. Pota, A. Lambert, S. Eckersley-Masun, and C. Farabet, "Visual Tracking and LIDAR Relative Positioning for Automated Launch and Recovery of an Unmanned Rotorcraft form Ships at Sea," in *Naval Engineers Journal*, **121 (2)**, 99–110 (2009).

4. Y. Gui, P. Guo, H. Zhang, Z. Lei, X. Zhou, J. Du, and Q. Yu, "Airborne Vision-Based Navigation Method for UAV Accuracy Landing Using Infrarred Lamps," in *Journal of Intelligent and Robotic Systems*, **72 (2)**, 197–219 (2013).
5. J. Gundlach, *Designing Unmanned Aircraft Systems: A Comprehensive Approach* (AIAA Education Series, 2013).
6. B. Herisse, T. Hamel, R. Mahony, and F.-X. Russotto, "The Landing Problem of a VTOL Unmanned Aerial Vehicle on a Moving Platform Using Optical Flow," in *Proceedings of IEEE/RSJ International Conference on Intelligent Robots and Systems*, 1600–1605 (2010).
7. S. Huh and D. H. Shim, "A Vision-Based Automatic Landing Method for Fixed-Wing UAVs," in *Journal of Intelligent and Robotic Systems*, **57**, 217–231 (2010).
8. H. J. Kim, M. Kim, H. Lim, C. Park, S. Yoon, D. Lee, H. Choi, G. Oh, J. Park, and Y. Kim, "Fully Autonomous Vision-Based Net-Recovery Landing System for a Fixed-Wing UAV," in *IEEE/ASME Transactions on Mechatronics*, **18 (4)**, 1–14 (2013).
9. *Leica ALS*60*: Airborne Laser Scanner Product Specifications*" (Leica Geosystems, 2008).
10. L. Marconi, A. Isidori, and A. Serrani, "Autonomous Vertical Landing on an Oscillating Platform: an Internal-Model Based Approach," in *Automatica*, **38 (1)**, 21–32 (2002).
11. T. Pérez and M. Blanke, *Simulation of Ship Motion in Seaway*, Technical Report EE03037 (2001).
12. T. S. Richardson, C. G. Jones, A. Likhoded, E. Sparks, I. Cowling, S. Willcox, and A. Jordan, "Automated Vision-based Recovery of a Rotatory Wing Unmanned Aerial Vehicle onto a Moving Platform," in *Journal of Field Robotics*, **30 (5)**, 667–684 (2013).
13. P. Riseborough, "Automatic Take-Off and Landing Control for Small UAV's," in *Proceedings of Asian Control Conference*, 754–762 (2004).
14. J. Rubio-Hervas, M. Reyhanoglu, and H. Tang, "Automatic Landing Control of Unmanned Aerial Vehicles on Moving Platforms," in *Proceedings 23rd IEEE International Symposium on Industrial Electronics*, 69–74 (2014).
15. J. L. Sanchez-Lopez, S. Saripalli, P. Campoy, J. Pestana, and C. Fu, "Toward Visual Autonomous Ship Board Landing of a VTOL UAV," in *Proceedings of International Conference on Unmanned Aircraft Systems*, 779–788 (2013).
16. O. Shakemia, M. Yi, T. J. Koo, and S. Sastry, "Landing an Unmanned Air Vehicle: Vision Based Motion Estimation and Nonlinear Control," in *Asian Journal of Control*, **1 (3)**, 128–145 (1999).
17. C. S. Sharp, O. Shakemia, and S. Sastry, "A Vision System for Landing an Unmanned Aerial Vehicle," in *Proceedings of IEEE International Conference on Robotics and Automation*, 1720–1727 (2001).
18. D. Simon, *Optimal State Estimation: Kalman, H_∞ and Nonlinear Approaches* (Winley, 2006).
19. SNAME, *Nomenclature for Treating the Motion of a Submerged Body Through a Fluid*, Technical Report Bulleting 1-5, Society of Naval Architects and Marine Engineers (1950).
20. G. A. Swift, "Model Identification and Control Design for the Lambda Unmanned Research Vehicle," Master's Thesis, Air Force Institute of Technology, WPAFB OH 45433-6583, 1991.
21. T. K. Venugopalan, T. Taher, and G. Barbastathis, "Autonomous Landing of an Unmanned Aerial Vehicle on an Autonomous Marine Vehicle," in *Proceedings of Oceans Conference*, 1–9 (2012).
22. X. Wang, G. Xu, Y. Tian, B. Wang, and J. Wang, "UAV's Automatic Landing in All Weather Based on the Cooperative Object and Computer Vision," in *Proceedings of International Conference on Instrumentation and Measurement, Computer, Communication and Control*, 1346–1351 (2012).
23. J. R. Wertz, *Spacecraft Attitude Determination and Control* (Kluwer Academic Publishers, 1978).
24. G. Xu, Y. Zhang, S. Ji, Y. Cheng, and Y. Tian, "Research on Computer Vision-Based for UAV Autonomous Landing on a Ship," *Pattern Recognition Letters*, **30 (6)** 600–605 (2009).
25. X. Zhou, Z. Lei, Q. Yu, H. Zhang, Y. Shang, J. Du, Y. Gui, and P. Guo, "Videometric Terminal Guidance Method and System for UAV Accurate Landing," in *Proceedings of SPIE*, **8387**, 31–51 (2012).